

# Physical quantity synergy in the field of turbulent heat transfer and its analysis for heat transfer enhancement

LIU Wei\*, LIU ZhiChun & HUANG SuYi

*School of Energy and Power Engineering, Huazhong University of Science and Technology, Wuhan 430074, China*

Received August 30, 2009; accepted November 20, 2009

Based on the principle of physical quantity synergy in the field of laminar heat transfer, and according to the models of zero equation and  $k$ - $\varepsilon$  two equations for the turbulent flow, the synergy equations for both energy and momentum conservation in the turbulent heat transfer are established. The synergy regulation among heat flux, mass flow and fluid driving force, and the mechanism of heat transfer enhancement it reflects are revealed. The synergy principle of physical quantity in the thermal flow field is extended from laminar flow to turbulent flow. The principle is verified to be universal by the calculation of heat transfer enhancement in a tube with an insert of helical twisted tape. Thus, corresponding to the synergy relation among physical quantities in the turbulent flow field, the performance of convective heat transfer and flow resistance for the tubes with different heat transfer components and surface can be compared through theoretical and computational analysis, which thereby provides a guidance for designing heat transfer units and heat exchangers.

**turbulent flow, physical quantity synergy, heat exchanger, heat transfer enhancement, performance evaluation**

**Citation:** Liu W, Liu Z C, Huang S Y. Physical quantity synergy in the field of turbulent heat transfer and its analysis for heat transfer enhancement. Chinese Sci Bull, 2010, 55: 2589–2597, doi: 10.1007/s11434-010-3009-7

Heat exchangers are widely applied to various industries such as power generation, petrochemistry, steel, metallurgy, refrigeration, cryogenic engineering, etc. The overall performance of the heat exchangers may be improved effectively by enhancing the convective heat transfer and reducing the flow resistance. The conventional heat transfer enhancement approach, however, only focuses on enhancing heat transfer. As a result, the fluid flow resistance often increases significantly [1,2]. The performance of heat exchangers may be further improved if more efforts are made to reduce the fluid flow resistance while maintaining certain heat transfer intensity. In addition, if the pump power consumption of the heat exchangers remains constant, reducing the flow resistance would increase the fluid velocity, thereby to achieve a better heat transfer effect. Therefore, reducing fluid friction resistance is another effective way to

enhance heat transfer.

In order to reveal the physical mechanism of heat transfer enhancement for the process of energy transfer in heat exchangers, Guo et al. [3] developed the field synergy principle for enhancing heat transfer from the energy equation. They suggested that physical performance of convective heat transfer would depend on the synergetic relation between its velocity field and heat-flux field. Under the same boundary conditions of velocity and temperature, the better the synergy between the velocity field and the heat-flux field was, the higher the heat transfer intensity would be. Some numerical computation and experiments in [4–19] verified that the field synergy principle could be used as a guide to design the heat transfer surface and heat exchangers. In addition, numerical computation in [20–22] showed that the synergic relations expressed in the field synergy principle were also suitable for turbulent heat transfer.

\*Corresponding author (email: w\_liu@hust.edu.cn)

### 1 Physical field quantity synergy for turbulent heat transfer

Based on the principle of field synergy for heat transfer enhancement, the physical quantity synergy in the laminar flow field is analyzed in [23,24] according to the physical mechanism of convective heat transfer between fluid and tube wall. Due to the random fluctuation of fluid particles in turbulence, the heat transfer mechanism between fluid and solid wall is more complex in turbulence than that in the laminar flow.

#### 1.1 Description of the turbulent flow

In general, physical quantities in turbulent flow can be expressed as the sum of time-averaged quantities and fluctuation quantities. If the Reynolds stress  $-\overline{\rho u'v'}$  caused by turbulence fluctuation in momentum equations is expressed in the form of shear stress similar to the laminar flow, whereas the turbulent fluctuation thermal diffusion  $-\overline{\rho c v'T'}$  in energy equation is also expressed in the similar form of laminar flow diffusion, then the two-dimensional boundary layer conservation equations in the Cartesian coordinates are

$$\frac{\partial(\rho u)}{\partial x} + \frac{\partial(\rho v)}{\partial y} = 0, \tag{1}$$

$$u \frac{\partial u}{\partial x} + v \frac{\partial u}{\partial y} = -\frac{1}{\rho} \frac{\partial p}{\partial x} + \frac{\partial}{\partial y} \left[ (v + \varepsilon_m) \frac{\partial u}{\partial y} \right], \tag{2}$$

$$u \frac{\partial T}{\partial x} + v \frac{\partial T}{\partial y} = \frac{\partial}{\partial y} \left[ (a + \varepsilon_h) \frac{\partial T}{\partial y} \right], \tag{3}$$

where  $\rho$  is the fluid density,  $v$  and  $\varepsilon_m$  are the molecular momentum diffusivity and the turbulent momentum diffusivity respectively,  $a$  and  $\varepsilon_h$  are the molecular thermal diffusivity and the turbulent thermal diffusivity respectively.

For momentum equations, taking into account the laminar shear stress caused by the molecular momentum transfer and turbulent shear stress caused by the momentum transfer due to turbulence fluctuation, the total shear stress is expressed as

$$\tau = \tau_l + \tau_t = \rho(v + \varepsilon_m) \frac{\partial u}{\partial y}, \tag{4}$$

where  $\tau_l$  and  $\tau_t$  are laminar and turbulent shear stress respectively. The turbulent momentum dissipation  $\varepsilon_m$  can be determined by mixing-length theory, i.e. zero-equation

model:  $\varepsilon_m = l_m^2 \left| \frac{du}{dy} \right|$ , where  $l_m$  is the mixing length which

characterizes the distance traveled by fluid particle before it becomes blended with neighboring particles. In this way, the Reynolds stress in eq. (2) can be expressed as

$$-\overline{\rho u'v'} = \rho \varepsilon_m \frac{du}{dy} = \rho l_m^2 \left| \frac{du}{dy} \right| \frac{du}{dy}. \tag{5}$$

In addition, according to  $k-\varepsilon$  two-equation turbulent model proposed by Jones and Launder [25,26], the Reynolds stress is stated as

$$-\overline{\rho u'v'} = \rho \varepsilon_m \frac{du}{dy} = c_\mu \frac{k^2}{\varepsilon} \frac{du}{dy}, \tag{6}$$

where the empirical constant  $c_\mu=0.09$ . The equation about the turbulent kinetic energy  $k$  is

$$u \frac{\partial k}{\partial x} + v \frac{\partial k}{\partial y} = \frac{\partial}{\partial y} \left[ \left( v + \frac{\varepsilon_m}{\sigma_k} \right) \frac{\partial k}{\partial y} \right] + \varepsilon_m \left( \frac{\partial u}{\partial y} \right)^2 - \varepsilon - 2v \left( \frac{\partial k^{1/2}}{\partial y} \right)^2. \tag{7}$$

The equation for turbulent dissipation rate  $\varepsilon$  is

$$u \frac{\partial \varepsilon}{\partial x} + v \frac{\partial \varepsilon}{\partial y} = \frac{\partial}{\partial y} \left[ \left( v + \frac{\varepsilon_m}{\sigma_\varepsilon} \right) \frac{\partial \varepsilon}{\partial y} \right] + c_1 \frac{\varepsilon}{k} \varepsilon_m \left( \frac{\partial u}{\partial y} \right)^2 - \frac{c_2 \varepsilon^2}{k} + 2\rho v \varepsilon_m \left( \frac{\partial^2 u}{\partial y^2} \right)^2. \tag{8}$$

In the above equations, when the Reynolds number is large, the empirical constants can be taken as  $c_1=1.45$ ,  $c_2=2$ ,  $\sigma_k=1$ ,  $\sigma_\varepsilon=1.3$ .

For the energy equation, the total heat transfer flux in the form of molecular diffusion and turbulent fluctuation is expressed as

$$q = q_l + q_t = -\rho c_p (a + \varepsilon_h) \frac{\partial T}{\partial y}, \tag{9}$$

where  $q_l$  and  $q_t$  are the thermal diffusion in laminar flow and turbulent flow defined in the form of Fourier heat conduction law respectively.

Eqs. (2) and (3) are very similar to the equations of the laminar boundary layer, so the synergy equations among turbulent physical quantities can be deduced from eqs. (2) and (3) by adopting similar approaches [23]. It is noteworthy that, when determining the turbulent momentum dissipation  $\varepsilon_m$ , either the zero-equation model or the two-equation model may be used. For the latter, although the Reynolds stress expression of eq. (6) changes, the nature of the turbulent momentum equation has not changed. So choosing different turbulence models will not affect theoretical derivation of the synergic equations for turbulent momentum.

#### 1.2 Characteristic of boundary layer for the turbulent flow

For the energy equation in the turbulent boundary layer, we have

$$\rho c_p \left( u \frac{\partial T}{\partial x} + v \frac{\partial T}{\partial y} \right) = \frac{\partial}{\partial y} \left[ (\lambda + \rho c_p \varepsilon_h) \frac{\partial T}{\partial y} \right], \quad (10)$$

where the total turbulent heat flux can be defined according to the Fourier heat conduction law:

$$q = -(\lambda + \rho c_p \varepsilon_h) \frac{\partial T}{\partial y} = -\lambda_t \frac{\partial T}{\partial y}. \quad (11)$$

So, for each fluctuation particle of fluid in the turbulent boundary layer, we have

$$\rho c_p \left( u \frac{\partial T}{\partial x} + v \frac{\partial T}{\partial y} \right) = \frac{\partial}{\partial y} \left( \lambda_t \frac{\partial T}{\partial y} \right). \quad (12)$$

Integrating eq. (12) along the  $y$  direction within the thermal boundary layer, we have

$$\int_0^{\delta_t} \rho c_p (\mathbf{U} \cdot \nabla T) dy = - \int_0^{\delta_t} \frac{\partial q}{\partial y} dy. \quad (13)$$

The turbulent heat transfer coefficient is defined by heat flux density in unit solid-wall area and temperature difference across the turbulent boundary layer, namely,

$$h_t = \frac{q_w}{T_w - T_f}, \quad (14)$$

where the fluid temperature  $T_f$  can be fluid temperature  $T_\infty$  or average temperature  $T_m$ , depending on different circumstances. Therefore, taking into account the temperature continuity between laminar substrate and the turbulent core area, for the unit area for heat transfer, integrating the right hand side of eq. (13) across the turbulent boundary layer yields:

$$\begin{aligned} \int_0^{\delta_t} \rho c_p (\mathbf{U} \cdot \nabla T) dy &= -q|_0^{\delta_t} = -\lambda_t \left. \frac{\partial T}{\partial y} \right|_w \\ &= q_w = h_t (T_w - T_m). \end{aligned} \quad (15)$$

As seen from the above expression, thermal energy transported by turbulent boundary layer is transferred through the solid walls, and the energy equations for laminar flow and turbulent flow are similar in form. However, for the turbulence problem, we need to define the turbulent Nusselt number, the turbulent Reynolds number and the turbulent Prandtl number according to the characteristics of the turbulent boundary layer:

$$Nu_t = \frac{h_t d}{\lambda + \rho c_p \varepsilon_h} = \frac{h_t d}{\lambda_t}, \quad (16)$$

$$Re_t = \frac{u_m d}{\nu + \varepsilon_m} = \frac{u_m d}{\nu_t}, \quad (17)$$

$$Pr_t = \frac{\nu + \varepsilon_m}{a + \varepsilon_h} = \frac{\nu_t}{a_t}, \quad (18)$$

where  $d$  is the characteristic length. Since  $\varepsilon_h$  and  $\varepsilon_m$  are not

the physical property parameters of fluid,  $\lambda_t$ ,  $\nu_t$  and  $a_t$  are defined as the turbulence equivalent thermal conductivity coefficient, the turbulent equivalent momentum diffusion coefficient and the turbulent equivalent thermal diffusion coefficient respectively.

In different regions of the turbulent flow field, turbulent  $Re_t$  and turbulent  $Pr_t$  can be simplified. In the laminar substrate,  $\varepsilon_m \ll \nu$ ,  $\varepsilon_h \ll \alpha$ , so  $Pr_t = \nu/\alpha$ ,  $Re_t = u_m d/\nu$ ; in the turbulent core area,  $\nu \ll \varepsilon_m$ ,  $\alpha \ll \varepsilon_h$ , so  $Pr_t = \varepsilon_m/\varepsilon_h$ ,  $Re_t = u_m d/\varepsilon_m$ .

### 1.3 Energy synergy equation

Consider the steady turbulent heat transfer in a two-dimensional parallel channel with height  $H$  and length  $L$ . For simplification, it is analyzed symmetrically by taking  $h=H/2$  channel length and the following dimensionless quantities are introduced,

$$Y = \frac{y}{h}, \quad \bar{\mathbf{U}} = \frac{\mathbf{U}}{u_m}, \quad \nabla \bar{T} = \frac{\nabla T}{(T_w - T_m)/h}, \quad T_w > T_\infty,$$

where  $h$  is the half-height of two-dimensional parallel channel,  $\mathbf{U}$  is the velocity vector,  $u_m$  is the fluid average velocity,  $T_w$  is the wall temperature,  $T_m$  is the average temperature for the fluid,  $T_\infty$  is the inflow fluid temperature. Thus, the non-dimensionless energy synergy equation can be obtained from eq. (5),

$$Nu_t = Re_t Pr_t \int_0^{\delta_t/h} (\bar{\mathbf{U}} \cdot \nabla \bar{T}) dY, \quad (19)$$

where the turbulent Nusselt number is  $Nu_t = \frac{h_t h}{\lambda_t}$ , turbulent

Reynolds number is  $Re_t = \frac{u_m h}{\nu_t}$ , the turbulent Prandtl number is

$Pr_t = \frac{\nu_t}{a_t} = \frac{\rho c_p \nu_t}{\lambda_t}$ . In fact, if the thermal boundary

layer merges in the center plane of channel, then integral limit becomes  $\delta/h=1$ , which means the channel flow becomes fully developed, thus eq. (19) can be applied to the whole channel.

In eq. (19), dot product of dimensionless velocity and dimensionless temperature gradient can be expressed as

$$\bar{\mathbf{U}} \cdot \nabla \bar{T} = |\bar{\mathbf{U}}| |\nabla \bar{T}| \cos \beta. \quad (20)$$

After substituting eq. (20) into eq. (19), it is known that dot product  $\bar{\mathbf{U}} \cdot \nabla \bar{T}$  increases with the decrease of synergy angle  $\beta$  between vectors  $\mathbf{U}$  and  $\nabla T$ . Obviously, the increase of dot product  $\bar{\mathbf{U}} \cdot \nabla \bar{T}$  means the increase of  $Nu_t$  number, and as a result, convective heat transfer between the fluid and the solid wall will be enhanced. The physical mechanism expressed by the synergy relations can be stated in this way: if the direction of fluid velocity is more close to that of heat flux, the effect of convective heat transfer will

be better in the turbulent flow field.

It is noteworthy that the above coordination mechanism in the turbulent heat flux field is not applicable for the reversed flow locations, because the heat can only transfer from positions with high temperature to positions with low temperature. Also, fluid temperature gradient in reversed flow zone does not change to the opposite direction, while the mass flow might point to the opposite direction of the mainstream.

#### 1.4 Momentum synergy equation

For the turbulent flow in the two-dimensional parallel channel mentioned above, its momentum conservation equation can be obtained by rewriting eq.(2):

$$\rho \left( u \frac{\partial u}{\partial x} + v \frac{\partial u}{\partial y} \right) = -\frac{\partial p}{\partial x} + \frac{\partial}{\partial y} \left( \rho \nu_t \frac{\partial u}{\partial y} \right). \quad (21)$$

Integrating the above equation along  $y$  direction within the boundary layer yields:

$$\begin{aligned} \int_0^\delta \rho (\mathbf{U} \cdot \nabla u) dy &= \int_0^\delta \frac{\partial p}{\partial x} dy - \frac{\partial}{\partial y} \left( \rho \nu_t \frac{\partial u}{\partial y} \right) dy \\ &= -\int_0^\delta \frac{\partial p}{\partial x} dy - \rho \nu_t \frac{\partial u}{\partial y} \Big|_w. \end{aligned} \quad (22)$$

By integrating eq.(22) along  $x$  direction from the channel inlet to its outlet, we obtain:

$$\int_0^L \int_0^\delta \rho (\mathbf{U} \cdot \nabla u) dx dy = -\int_0^L \int_0^\delta \frac{\partial p}{\partial x} dx dy - \int_0^L \tau_w dx, \quad (23)$$

where  $\tau_w$  is the turbulent shear stress of wall, and it can be expressed as

$$\int_0^L \tau_w dx = \int_0^{L_e} \tau_{w_1} dx + \int_{L_e}^L \tau_{w_2} dx, \quad (24)$$

where  $\tau_{w_1}$  and  $\tau_{w_2}$  represent the shear stress in the channel entrance region and the fully developed turbulent flow region respectively. According to [27], we can obtain  $\tau_{w_1}$  and  $\tau_{w_2}$  as

$$\tau_{w_1} = \frac{0.019 \rho u_m^2}{Re_t^{0.2} (x/h)^{0.2}}, \quad x < L_e, \quad (25)$$

$$\tau_{w_2} = \frac{0.079 \rho u_m^2}{Re_t^{0.25}}, \quad x \geq L_e, \quad (26)$$

where  $L_e$  stands for the length of the channel entrance region.

Substituting eqs. (24)–(26) into eq. (23), we have

$$\begin{aligned} \int_0^L \int_0^\delta \rho (\mathbf{U} \cdot \nabla u) dx dy &= -\int_0^L \int_0^\delta \frac{\partial p}{\partial x} dx dy \\ &= -\frac{0.024 \rho u_m^2 L_e}{Re_t^{0.2} (L_e/h)^{0.2}} - \frac{0.079 \rho u_m^2 (L - L_e)}{Re_t^{0.25}}. \end{aligned} \quad (27)$$

The dimensionless numbers are introduced as

$$\begin{aligned} X &= \frac{x}{L}, \quad Y = \frac{y}{h}, \quad \bar{\mathbf{U}} = \frac{\mathbf{U}}{u_m}, \quad \bar{u} = \frac{u}{u_m}, \\ Eu_t &= \Delta \bar{p} = \frac{\Delta p}{\rho u_m^2}, \quad \chi_1 = \frac{L_e}{L}, \\ \chi_2 &= \frac{L - L_e}{L}, \quad \Lambda = \frac{L_e}{H}, \quad \nabla \bar{u} = \frac{\left( \frac{\partial}{\partial x} \mathbf{i} + \frac{\partial}{\partial y} \mathbf{j} \right) u}{u_m/h}, \\ \nabla \bar{p} &= \frac{\left( \frac{\partial}{\partial x} \mathbf{i} + \frac{\partial}{\partial y} \mathbf{j} \right) p}{\rho u_m^2/h}, \quad \frac{\partial}{\partial y} \mathbf{j} = 0, \end{aligned}$$

where  $Eu_t$  refers to the turbulent Euler number;  $\Delta p$  refers to the pressure drop between the channel inlet and outlet;  $\chi_1$  and  $\chi_2$  are the length percentage of entrance region and the full developed region respectively;  $\Lambda$  is the ratio of the entrance length to channel height;  $i$  and  $j$  refer to unit vectors of  $x$  and  $y$  coordinates respectively.

After dimensionless treatment, eq. (27) can be expressed as

$$\begin{aligned} \int_0^1 \int_0^{\delta/h} (\bar{\mathbf{U}} \cdot \nabla \bar{u}) dXdY &= -\int_0^1 \int_0^{\delta/h} (\nabla \bar{p} \cdot \mathbf{I}) dXdY \\ &= -\frac{0.021 \chi_1}{(\Lambda Re_t)^{0.2}} - \frac{0.079 \chi_2}{Re_t^{0.25}}, \end{aligned} \quad (28)$$

where  $\delta/h$  refers to dimensionless thickness of the velocity boundary layer. If the velocity boundary layer merges in the center plane of the channel, integral limit becomes  $\delta/h=1$ , which means the channel turbulent flow becomes fully developed.  $\mathbf{I}$  refers to unit vector. The integral term on the right-hand side of eq. (28) refers to dimensionless pressure drop for the parallel channel with height  $h=H/2$ , which can be expressed as

$$\Delta \bar{p} = -\int_0^1 \int_0^{\delta/h} (\nabla \bar{p} \cdot \mathbf{I}) dXdY. \quad (29)$$

From eqs. (28) and (29), an expression for dimensionless momentum synergy equation can be deduced:

$$Eu_t = \frac{0.021 \chi_1}{(\Lambda Re_t)^{0.2}} + \frac{0.079 \chi_2}{Re_t^{0.25}} + \int_0^1 \int_0^{\delta/h} (\bar{\mathbf{U}} \cdot \nabla \bar{u}) dXdY, \quad (30)$$

where dot product of dimensionless velocity and the dimensionless velocity gradient can be expressed as

$$\bar{\mathbf{U}} \cdot \nabla \bar{u} = |\bar{\mathbf{U}}| |\nabla \bar{u}| \cos \alpha. \quad (31)$$

After substituting eq. (31) into eq. (30), we can find that dot product  $\bar{\mathbf{U}} \cdot \nabla \bar{u}$  decreases with the increase of synergy angle  $\alpha$  between vectors  $\mathbf{U}$  and  $\nabla u$ . But it can be noted

that the decrease of dot product  $\bar{U} \cdot \nabla \bar{u}$  leads to the decrease of the  $Eu_t$  number, and as a result, the flow resistance of fluid will decrease. Obviously, focusing on improving the synergy relations may be a new direction for reducing fluid friction resistance, which is important for designing heat exchangers for lower flow resistance.

### 1.5 Evaluation of heat transfer enhancement

In the traditional heat transfer method, heat transfer is enhanced but with a cost of the increase of flow resistance, especially in the turbulence zone. Under some circumstances, when the increase of flow resistance is too large, heat transfer may not be enhanced; on the contrary, if the flow resistance and power consumption are smaller, the fluid flow conditions in heat exchanger are better, and as a result, heat transfer efficiency will be improved accordingly. Therefore, two aspects of the heat transfer enhancement design for heat transfer should be considered: (1) enhancing convective heat transfer; and (2) reducing flow resistance. In order to evaluate the comprehensive performance of heat transfer enhancement, the following formula can be used:

$$PEC = \frac{Nu_t / Nu_{t0}}{(f / f_0)^{1/3}}, \quad (32)$$

where  $Nu_t$  and  $Nu_{t0}$  are the turbulent Nusselt numbers for enhanced tube and bare tube respectively,  $f$  and  $f_0$  are the friction coefficients for enhanced tube and bare tube respectively.

On the basis of analyzing the vector quantities relation in the non-isothermal laminar flow field, Liu et al. [23] set up the synergy relation among the velocity vector  $U$ , velocity gradient  $\nabla u$ , temperature gradient  $\nabla T$  and pressure gradient  $\nabla p$ . From the turbulent synergy equations of eqs. (19) and (30), it can be obtained that the vector quantities in turbulent flow should also meet the synergy relationship. Therefore, the synergy angle between  $\nabla T$  and  $\nabla u$  can be expressed as

$$\gamma = \arccos \frac{\nabla T \cdot \nabla u}{|\nabla T| |\nabla u|}. \quad (33)$$

From the synergy angles  $\alpha$ ,  $\beta$  and  $\gamma$  of fluid particles in the turbulent convective field, it can be obtained that smaller synergy angle  $\beta$  and larger  $\alpha$  will result in larger synergy angle  $\gamma$ . As a result, it can be induced that synergy angle  $\gamma$  can reveal the extent of heat transfer enhancement and flow resistance reduction. That is to say, the larger angle  $\gamma$  is, the better the comprehensive performance of the heat exchanger would be. Therefore, angle  $\gamma$  can be seen as a criterion for evaluating heat transfer enhancement.

In the same way, the synergy angle between velocity  $U$  and pressure gradient  $\nabla p$  can be expressed as

$$\theta = \arccos \frac{U \cdot \nabla p}{|U| |\nabla p|}. \quad (34)$$

As shown in eq. (34), the smaller the synergy angle  $\theta$  is, the better the synergy between  $U$  and  $\nabla p$  would be, and the better the coordination between mass flow and driving potential would be, which would result in the decrease of flow resistance. As far as flow resistance reduction is concerned, although physical meanings of eqs. (31) and (34) are the same, the latter is more intuitive for understanding the flow resistance reducing mechanisms. It is obvious that improving the synergy relation can reduce the flow resistance.

Figure 1 shows the synergy relation of physical quantities of fluid particle. In the figure,  $u\mathbf{i}$ ,  $v\mathbf{j}$  and  $w\mathbf{k}$  are the components of velocity vector  $U$  in  $x$ ,  $y$  and  $z$  direction respectively,  $\nabla u = \frac{\partial u}{\partial x} \mathbf{i} + \frac{\partial u}{\partial y} \mathbf{j} + \frac{\partial u}{\partial z} \mathbf{k}$  is the velocity gradient in  $x$  direction. It can be seen in the figure that intersection angles of  $\nabla u$  with  $U$ ,  $\nabla T$ , and  $\nabla p$  are all smaller than  $90^\circ$ . Therefore,  $\nabla u$  can be used as a reference vector when characterizing the synergy relation between vector physical quantities  $U$ ,  $\nabla T$  and  $\nabla p$ .

The above analysis suggests that there exists a specific relation between physical quantity synergy and heat transfer enhancement in the non-isothermal turbulent flow field. If the physical quantities of all fluid particles satisfy the synergy relation, turbulent heat transfer will be enhanced and flow resistance will be reduced, and as a result, enhanced heat transfer will be achieved.

## 2 Calculation and analysis for heat transfer enhancement

Based on the physical model in which helical twisted tape for disturbing fluid is interpolated in a tube, numerical verification for the synergy principle among physical quantities is

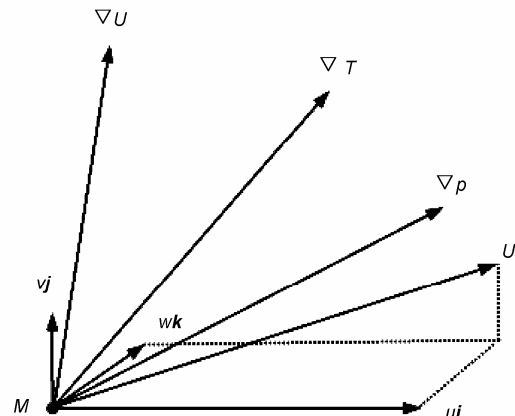


Figure 1 The diagram of vector relation at a fluid particle  $M$  among velocity, velocity gradient, temperature gradient and pressure gradient.

carried out.

In order to strengthen temperature distribution uniformity or increase fluid disturbance, a helical twisted tape is designed as shown in Figure 2.

**2.1 Mathematical model**

From the physical model shown in Figure 2, the RNG *k-ε* model combined with mass, momentum and energy conservation equations is employed to numerically simulate the flow and heat transfer. The following assumptions are made to establish the mathematical model: (1) The physical properties of fluid are constant; (2) The fluid is incompressible, isotropic and continuous; (3) The fluid is Newton fluid; and (4) The effect of gravity can be ignored. The common equations for flow and heat transfer are expressed as [28]

$$\frac{\partial(\rho u_i \Phi)}{\partial x_i} = \frac{\partial}{\partial x_j} \left( \Gamma \frac{\partial \Phi}{\partial x_j} \right) + S. \tag{35}$$

The turbulent kinetic energy *k* and the dissipation rate *ε* for RNG *k-ε* turbulence model are obtained from the following transport equations:

$$\frac{\partial(\rho k u_i)}{\partial x_i} = \frac{\partial}{\partial x_j} \left( \alpha_k \mu_{eff} \frac{\partial k}{\partial x_j} \right) + G_k + \rho \varepsilon, \tag{36}$$

$$\frac{\partial(\rho \varepsilon u_i)}{\partial x_i} = \frac{\partial}{\partial x_j} \left( \alpha_\varepsilon \mu_{eff} \frac{\partial \varepsilon}{\partial x_j} \right) + \frac{C_{1\varepsilon}^*}{k} G_k - C_{2\varepsilon} \rho \frac{\varepsilon^2}{k}. \tag{37}$$

In the above equations, for the continuity equation,  $\Phi=1, \Gamma=0, S=0$ ; for the momentum equation,  $\Phi=u, v, w, \Gamma=\mu_{eff}=\mu+\mu_t, S=-\frac{\partial p}{\partial x_i} + \frac{\partial}{\partial x_j} \left( \mu_{eff} \frac{\partial u_i}{\partial x_j} \right)$ ; for the energy equation,  $\Phi=T, \Gamma = \frac{\mu}{Pr} + \frac{\mu_t}{\sigma_T}, S=0, \mu_t = \rho C_{\mu} \mu \frac{k^2}{\varepsilon}, C_{\mu} = 0.0845, \alpha_k = \alpha_\varepsilon = 1.39, C_{1\varepsilon}^* = C_{1\varepsilon} \frac{\eta(1-\eta/\eta_0)}{1+\beta\eta^2}, C_{1\varepsilon} = 1.42, C_{2\varepsilon} = 1.68, \eta = (2E_{ij} \cdot E_{ij})^{1/2} \frac{k}{\varepsilon}$ ,

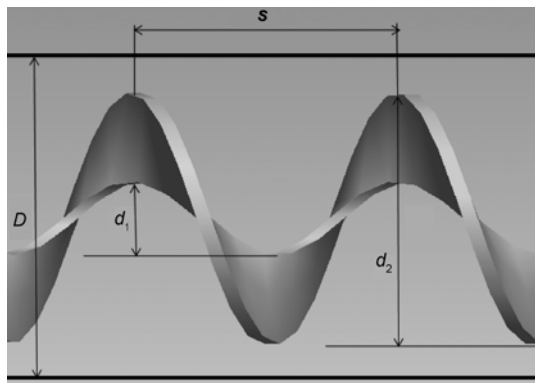


**Figure 2** The physical model of heat-transfer enhanced tube with an insert of helical twisted tape.

$$E_{ij} = \frac{1}{2} \left( \frac{\partial u_i}{\partial x_j} + \frac{\partial u_j}{\partial x_i} \right), \quad \eta_0=4.377, \quad \beta=0.012,$$

where  $\mu$  is the dynamic viscosity, *Pr* is the fluid Prandtl number,  $\sigma_T$  is the turbulence Prandtl number, *p* is the fluid pressure, *T* is the fluid temperature,  $\mu, v$  and *w* are the velocity components, *Γ* is the generalized diffusion coefficient,  $\Phi$  is the universal variable, and *S* is the source item.

To solve the above governing equations, SIMPLEC algorithm was used for pressure-velocity coupling, and QUICK scheme was chosen to discretize momentum equation and energy equations. The wall function method was used to treat the near-wall region.

**2.2 Results and discussion**

For the physical model shown in Figure 2, the parameters for computation are set as follows: Tube length *L*=1500 mm, tube diameter *D*=25 mm, inner diameter of helical twisted tape *d*<sub>1</sub>=5 mm, outer diameter *d*<sub>2</sub>=20 mm, tape width *W*=*d*<sub>2</sub>−*d*<sub>1</sub>=15 mm, tape thickness *t*=1 mm, pitch *s*=18 mm. In this study, water is used as the fluid, and the inlet temperature is 353 K, wall temperature is set at 298 K.

Figures 3 and 4 show the calculation results for the enhanced tube with the helical twisted tape inserted. From the figures it can be seen that the Nusselt number of the enhanced tube is 1–1.2 times larger than that of the bare tube in the Reynolds number of 6000 to 12000, while the increase of the flow resistance of the former is only about 30% higher than that of the latter, which indicates that the helical twisted tape is an ideal heat transfer component with high heat transfer efficiency and low flow resistance. Figure 2 shows the comparison of PEC for the enhancing tube and bare tube. From the figure it can be observed that the increase of the amplitude of PEC value for the enhanced tube is significant and the value is about 2.

Figure 6 shows the comparison of averaging synergy angle  $\beta$  for the enhanced tube and the bare tube. It can be found that the average synergy angle  $\beta$  is much smaller than

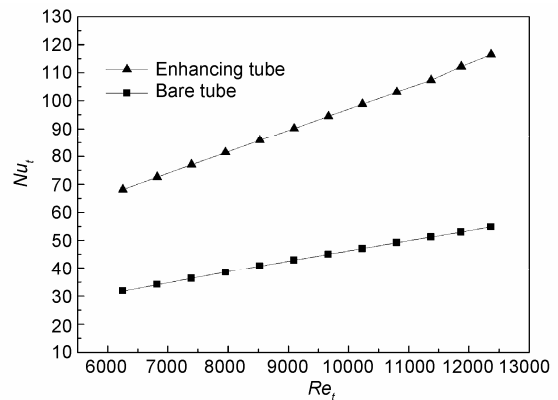


**Figure 3** The variation of *Nu<sub>t</sub>* number with *Re<sub>t</sub>* number for heat-transfer enhanced tube with helical twisted tape and bare tube.

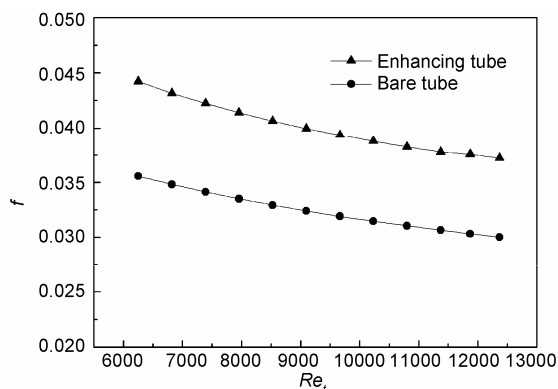


**Figure 4** The variation of resistance coefficient  $f$  with  $Re_t$  number for heat-transfer enhanced tube with helical twisted tape and bare tube.

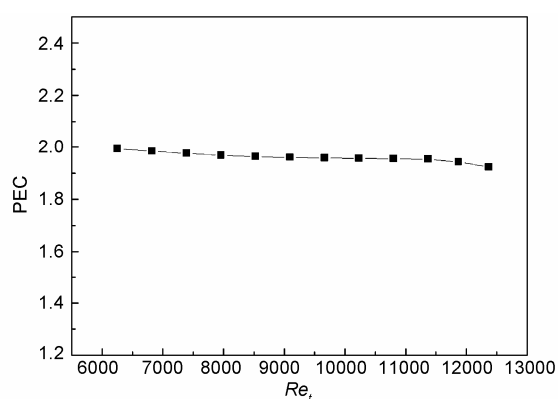


**Figure 5** The variation of PEC value with  $Re_t$  number for heat-transfer enhanced tube with helical twisted tape and bare tube.

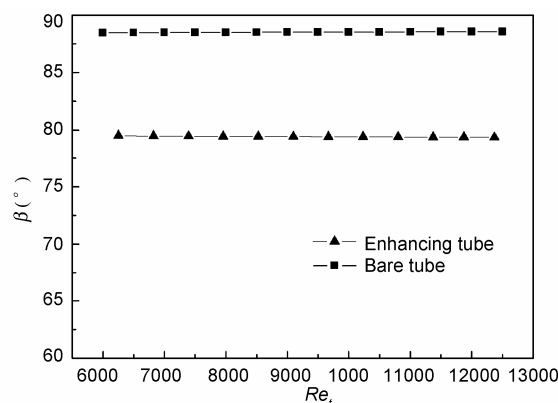


**Figure 6** The variation of average synergy angle  $\beta$  with  $Re_t$  number for heat-transfer enhanced tube with helical twisted tape and bare tube

that of the bare tube, which indicates that the heat transfer efficiency increases significantly, an outcome that is consistent with the calculation results shown in Figure 3. Of course, for higher heat transfer enhancement requests, we can optimize the structure and size of the helical twisted tape to further reduce the average angle  $\beta$ , improve the disturbance effect, and increase the heat transfer intensity.

Figures 7 and 8 show the comparisons between the synergy angles  $\alpha$  and  $\theta$  for the enhanced heat transfer tube and the bare tube. As shown in Figure 7, when the bare tube is replaced by the enhanced tube, the average synergy angle  $\alpha$  decreases from  $86^\circ$  to  $64^\circ$ ; consequently, the flow resistance will increase. But the increase of flow resistance is not particularly large, and its growth rate is smaller than that of the Nusselt number. In addition, as shown in Figure 8, the average synergy angle increases from  $1^\circ$  as in the bare tube to approximately  $55^\circ$  as in the enhanced tube, which suggests that, after inserting the helical twisted tape, the direction of the mass-flow driven force in the turbulent flow field is deviated. As a result, the flow resistance increases. Therefore, synergy angle  $\theta$  may be used to evaluate flow resistance reduction, which is similar to the case in which synergy angle  $\beta$  is used to evaluate heat transfer enhancement.

Figure 9 shows the comparison between the average synergy angles  $\gamma$  for the helical twisted tape inserted tube and the bare tube. As shown in the figure, the synergy angle  $\gamma$  of the bare tube is small (about  $5^\circ$ ), indicating that there is no enhancing effect. For the enhanced tube, the average angle

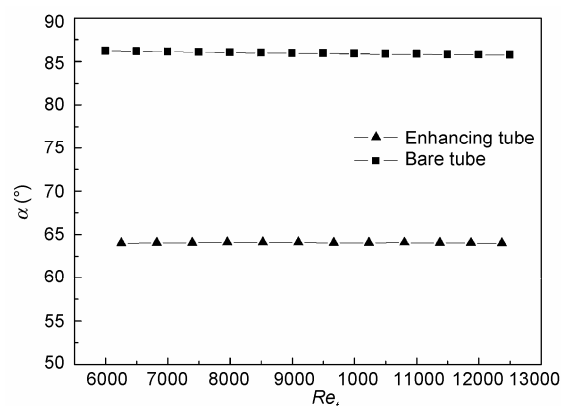


**Figure 7** The variation of average synergy angle  $\alpha$  with  $Re_t$  number for heat-transfer enhanced tube with helical twisted tape and bare tube.

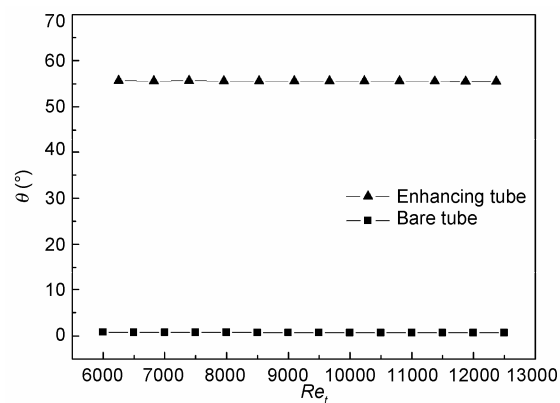


**Figure 8** The variation of average synergy angle  $\theta$  with  $Re_t$  number for heat-transfer enhanced tube with helical twisted tape and bare tube.

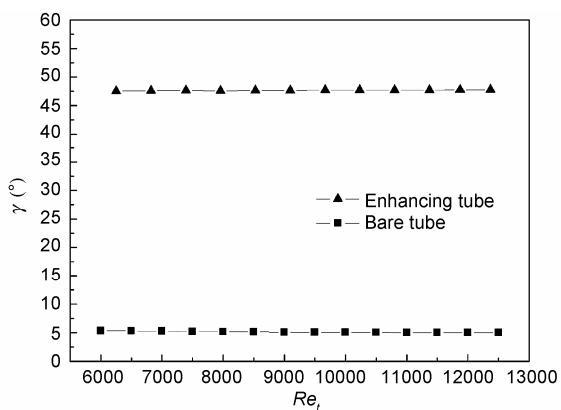


**Figure 9** The variation of average synergy angle  $\gamma$  with  $Re_t$  number for heat-transfer enhanced tube with helical twisted tape and bare tube.

exceeds  $47^\circ$ , which is about 8 times larger than that of the bare tube, indicating an excellent comprehensive performance of heat exchange enhancement. Therefore, the helical twisted tape is a recommendable heat transfer unit tube and can be applied to heat transfer enhancement of tube side in various types of heat exchangers, such as shell-and-tube heat exchangers, tubular heat exchangers and jacket-tube heat exchangers, for energy conservation.

### 3 Conclusions

This paper first defines the turbulence equivalent thermal conductivity, turbulence equivalent thermal diffusion coefficient and turbulence equivalent momentum diffusion coefficient according to turbulent model and characteristics of the boundary layer. Then, it establishes turbulent synergy equations for energy and momentum transfer, and describes the synergy relations among heat flow, mass flow and driving force in the turbulence flow field, which reveals the relations between the physical quantities synergy and the heat transfer enhancement. The principle of physical quantity synergy is also extended for heat transfer enhancement from the laminar flow to the turbulence flow.

The synergy angles  $\alpha$ ,  $\beta$  and  $\gamma$  in the turbulent flow field of convective heat transfer can reveal the heat transfer enhancement intensities. The smaller the synergy angle  $\alpha$  is, the lower the flow resistance coefficient  $f$  will be, and the smaller the pressure drop will be correspondingly; the smaller the synergy angle  $\beta$  is, the bigger the heat transfer coefficient  $h_t$  will be, which means convective heat transfer between the fluid and the tube wall will be stronger. The bigger the synergy angle  $\gamma$  is, the higher the PEC value will be. This means the comprehensive performance of a heat transfer unit will be improved.

When the Reynolds number is within the range of 6000–12000, the average synergy angle  $\alpha$  of helical twisted tape is about  $64^\circ$ , and compared with the bare tube the in-

crease of flow resistance is about 30%. For heat transfer, the average synergy angle  $\beta$  of helical twisted tape is about  $80^\circ$ . Compared with the bare tube, the heat transfer coefficient increases by 100%–120%. The average synergy angle  $\gamma$  is about  $47^\circ$ , and the PEC value is close to 2. As seen above, the increase in the rate of flow resistance is less than that of the heat transfer for the helical twisted tape inserted tube. Meanwhile, the PEC value is higher. Therefore, the enhanced tube is a heat transfer component with high comprehensive performance.

*This work was supported by the National Basic Research Program of China (2007CB206903) and the National Natural Science Foundation of China (50721005).*

- 1 Webb R L. Principles of Enhanced Heat Transfer. New York: Wiley, 1994
- 2 Bergles A E. ExHFT for fourth generation heat transfer technology. *Exp Therm Fluid Sci*, 2002, 26: 335–344
- 3 Guo Z Y, Li D Y, Wang B X. A novel concept for convective heat transfer enhancement. *Int J Heat Mass Transfer*, 1998, 41: 2221–2225
- 4 Zhao T S, Song Y J. Forced convection in a porous medium heated by permeable wall perpendicular to flow direction: Analyses and measurements. *Int J Heat Mass Transfer*, 2001, 44: 1031–1037
- 5 Tao W Q, Guo Z Y, Wang B X. Field synergy principle for enhancing convective heat transfer—its extension and numerical verification. *Int J Heat Mass Transfer*, 2002, 45: 3849–3856
- 6 Tao W Q, He Y L, Wang Q W, et al. A unified analysis on enhancing single phase convective heat transfer with field synergy principle. *Int J Heat Mass Transfer*, 2002, 45: 4871–4879
- 7 Shen S, Liu W, Tao W Q. Analysis of field synergy on natural convective heat transfer in porous media. *Int Comm Heat Mass Transfer*, 2003, 30: 1081–1090
- 8 Tao W Q, He Y L, Qu Z G, et al. Application of the field synergy principle in developing new type heat transfer enhanced surfaces. *J Enhanc Heat Transfer*, 2004, 11: 433–449
- 9 Qu Z G, Tao W Q, He Y L. Three-dimensional numerical simulation on laminar heat transfer and fluid flow characteristics of strip fin surface with X-arrangement of strips. *J Heat Transfer*, 2004, 126: 697–707
- 10 Cheng Y P, Qu Z G, Tao W Q, et al. Numerical design of efficient slotted fin surface based on the field synergy principle. *Numer Heat Transfer A*, 2004, 45: 517–538
- 11 Chen W L, Guo Z Y, Chen C K. A numerical study on the flow over a novel tube for heat transfer enhancement with linear eddy-viscosity model. *Int J Heat Mass Transfer*, 2004, 47: 3431–3439
- 12 He Y L, Tao W Q, Song F Q, et al. Three-dimensional numerical study of heat transfer characteristics of plain plate fin-and-tube heat exchangers from view point of field synergy principle. *Int J Heat Fluid Flow*, 2005, 6: 459–473
- 13 Guo Z Y, Tao W Q, Shah R K. The field synergy (coordination) principle and its applications in enhancing single phase convective heat transfer. *Int J Heat Mass Transfer*, 2005, 48: 1797–1807
- 14 Chen C K, Yen T Z, Yang Y T. Lattice Boltzmann method simulation of backward-facing step on convective heat transfer with field synergy principle. *Int J Heat Mass Transfer*, 2006, 49: 1195–1204
- 15 Ma L D, Li Z Y, Tao W Q. Experimental verification of the field synergy principle. *Int Comm Heat Mass Transfer*, 2007, 34: 269–276
- 16 Wu J M, Tao W Q. Investigation on laminar convection heat transfer in fin-and-tube heat exchanger in aligned arrangement with longitudinal vortex generator from the viewpoint of field synergy principle. *Appl Therm Eng*, 2007, 27: 2609–2617
- 17 Cai R X, Gou C H. Discussion of the convective heat transfer and field synergy principle. *Int J Heat Mass Transfer*, 2007, 50: 5168–5176
- 18 Cheng Y P, Lee T S, Low H T. Numerical simulation of conjugate

- heat transfer in electronic cooling and analysis based on field synergy principle. *Appl Therm Eng*, 2008, 28: 1826–1833
- 19 Chen Q, Ren J X, Guo Z Y. Fluid flow field synergy principle and its application to drag reduction. *Chinese Sci Bull*, 2008, 53: 1768–1772
- 20 Chen Q, Ren J X, Meng J A. Field synergy equation for turbulent heat transfer and its application. *Int J Heat Mass Transfer*, 2007, 50: 5334–5339
- 21 Zeng M, Tao W Q. Numerical verification of the field synergy principle for turbulent flow. *J Enhanc Heat Transfer*, 2004, 11: 451–457
- 22 Meng J A, Liang X G, Li Z X. Field synergy optimization and enhanced heat transfer by multi-longitudinal vortexes flow in tube. *Int J Heat Mass Transfer*, 2005, 48: 3331–3337
- 23 Liu W, Liu Z C, Guo Z Y. Physical quantity synergy in laminar flow field of convective heat transfer and analysis of heat transfer enhancement. *Chinese Sci Bull*, 2009, 54: 3579–3586
- 24 Liu W, Liu Z C, Ming T Z, et al. Physical quantity synergy in laminar flow field and its application in heat transfer enhancement. *Int J Heat Mass Transfer*, 2009, 52: 4669–4672
- 25 Jones W P, Launder B E. The prediction of laminarization with a two-equation model of turbulence. *Int J Heat Mass Transfer*, 1972, 15: 301–311
- 26 Jones W P, Launder B E. The calculation of low-Reynolds-number phenomena with a two-equation model of turbulence. *Int J Heat Mass Transfer*, 1973, 16: 1119–1130
- 27 Oertel H. *Prandtl's Essentials of Fluid Mechanics*. New York: Springer, 2004
- 28 Patankar S V. *Numerical Heat Transfer and Fluid Flow*. New York: McGraw-Hill, 1980